# Screening of Magnetic Nanoparticles for Magnetic Hyperthermia Application by Finite Element Method

**Jose Hernandez-Romero, Chemical and Materials Engineering**

Mentor: Dr. Huseyin Ucar

Kellogg Honors College Capstone Project

CPP Student RSCA Conference 2022

## I. Introduction

- Attainability of large alternating magnetic field (AMF) heating rates is essential for a magnetic fluid to be used in various applications that require localized heating in a controllable manner.
- In recent years, the application of magnetic nanoparticles (MNPs) has sparked great interest for the application of large alternating magnetic fields (AMF) in drug delivery and many cancer treatments.
- Currently, radiation therapy has been the standard treatment for cancer since the discovery of X-rays by Roentgen [1].
- Radiation therapy is typically used in combination with surgeries or chemotherapies, and its success is dependent on the tumor's radio-resistance and normal tissue toxicity, which determines the appropriate dosage to administer for treatment [1].
- Alternatively, for solid tumors, chemotherapy has been used most effectively as a secondary method to surgery and radiation therapy [2].
- Magnetic hyperthermia involves elevating the temperature of a tumor region to approximately 42-46℃ for an extended period of time, from which it may induce apoptosis in cancer cells [3].
- As MNPs are injected into a tumor site and an AMF field is applied, the magnetic energy is converted to heat via relaxation losses allowing the cancer cells to be damaged with minimal injury to the normal tissue [4].
- Eddy currents, hysteresis, and resonance losses are negligible to the heat generation in MNPs due to the small size of particles (< 15 nm) [5].
- Specific loss power (SLP), which is the heat generated per unit mass of MNPs, and the MNPs' concentration, helps govern the temperature enhancement induced by the MNPs [3].
- Magnetic parameters that govern the heating efficiency of the magnetic nanoparticles include the magnetic anisotropy (K), saturation magnetization ($M_s$), and the size of the MNPs.

## II. Objective

In this study, a 3D thermo-fluid model in COMSOL Multiphysics was generated to analyze the thermal effect of localized heating by six different magnetic nanoparticles on the temperature distribution of a liver tumor. Furthermore, the relationship between particle dosage and the fraction of tumor damage was investigated.

## III. 3D Model and Mathematical Formulation

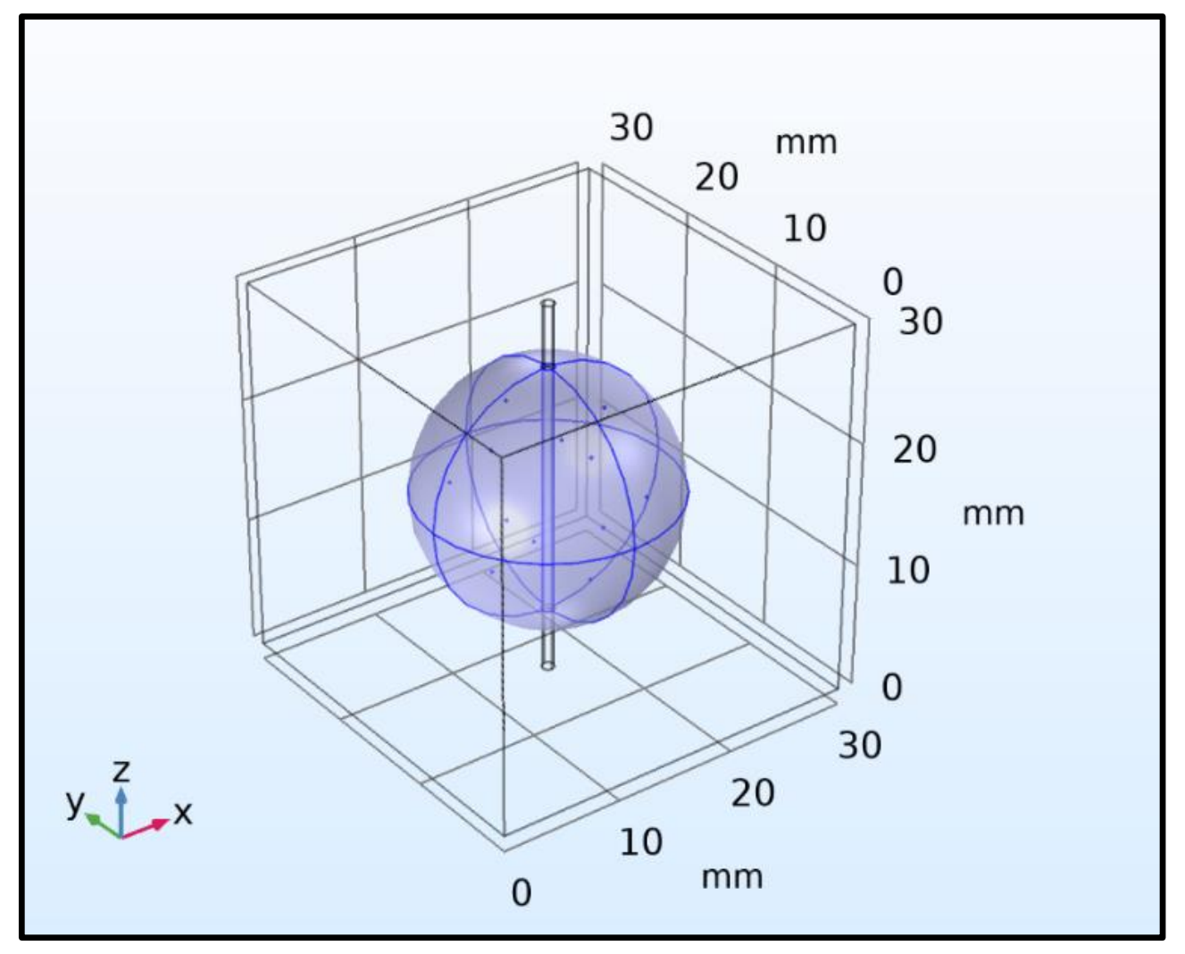

- **Specific Loss Power (SLP):**

$$SLP = \mu_0 \pi \chi_0 f \frac{2\pi f \tau_R}{1+(2\pi f \tau_R)^2} H^2$$

- **Effective Relaxation Time:**

$$\tau_R = \frac{(\tau_N * \tau_B)}{(\tau_N + \tau_B)}; \tau_N = \tau_0 e^{\frac{KV_m}{k_B T}} \text{ and } \tau_B = \frac{3\eta V_H}{k_B T}$$

- **Pennes' Bioheat Equation:**

$$\rho_i c_i \frac{\partial T_i}{\partial t} + \nabla \cdot (-k_i \nabla T_i) = \rho_b c_b \omega_b (T_b - T_i) + Q_i + Q$$

- **Navier-Stokes Equation:**

$$\rho_b c_b \left(\frac{\partial T_b}{\partial t} + v_z \frac{\partial T_b}{\partial z}\right) = \nabla \cdot (k_b \nabla T_b) + Q$$

- The Finite Element Method was used to solve the bioheat transport equation, where a system of equations was obtained as a function of temperature
- 12 injection sites were made depicting magnetic nanoparticles each with a 0.1 mm radius
- A blood vessel was placed in the center of the model with a 0.5 mm radius and 30 mm height
- The MNPs were set at a volume concentration of 0.1 with a particle radius of 0.1 mm and an initial particle dosage of 0.5 kg/m³ was used
- The time of interest for each study was 1500 seconds, and a Normal mesh type was used

## IV. Results and Discussion

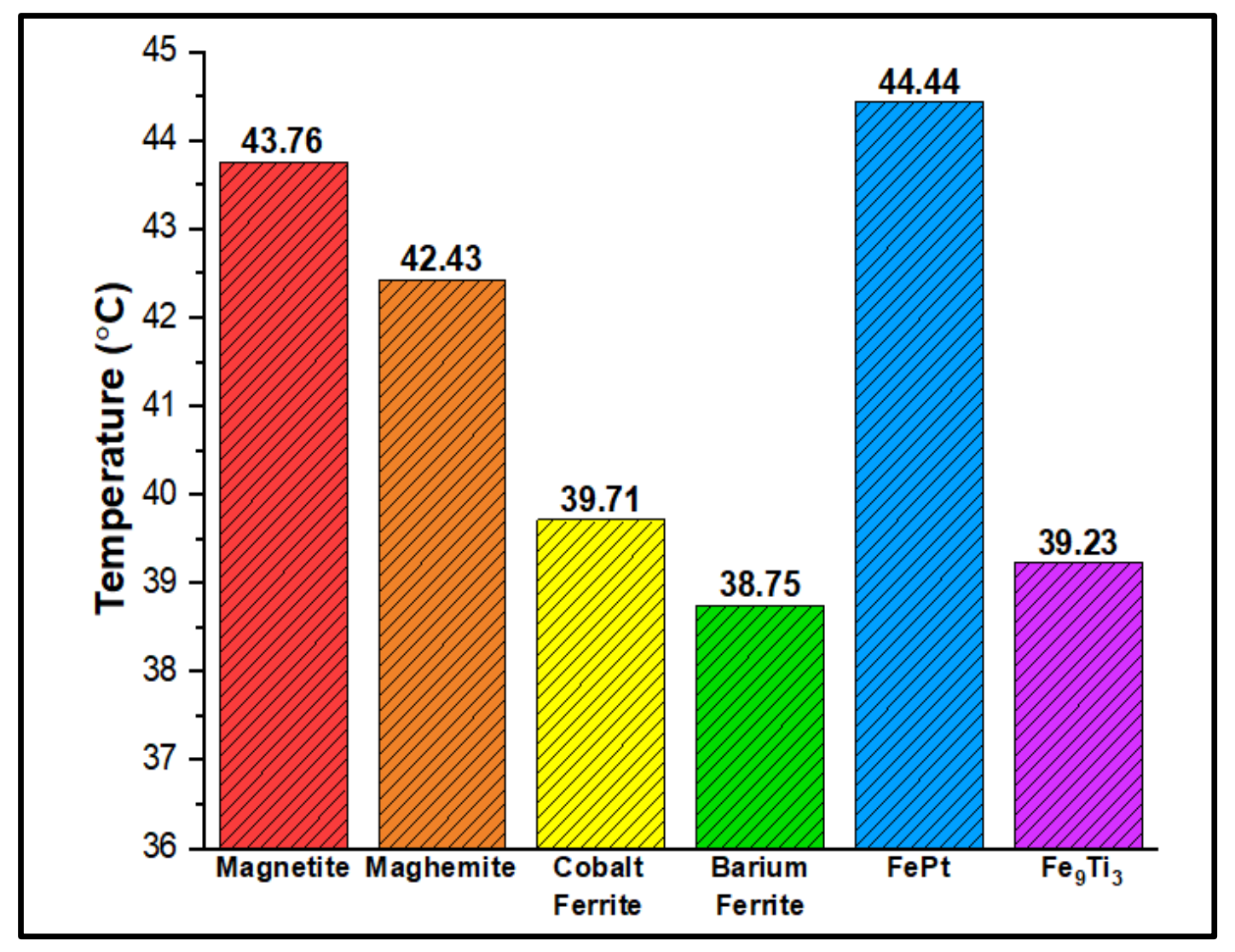

**Figure 1:** Maximum Heat Concentration of all MNPs at Tumor for 1500 sec.

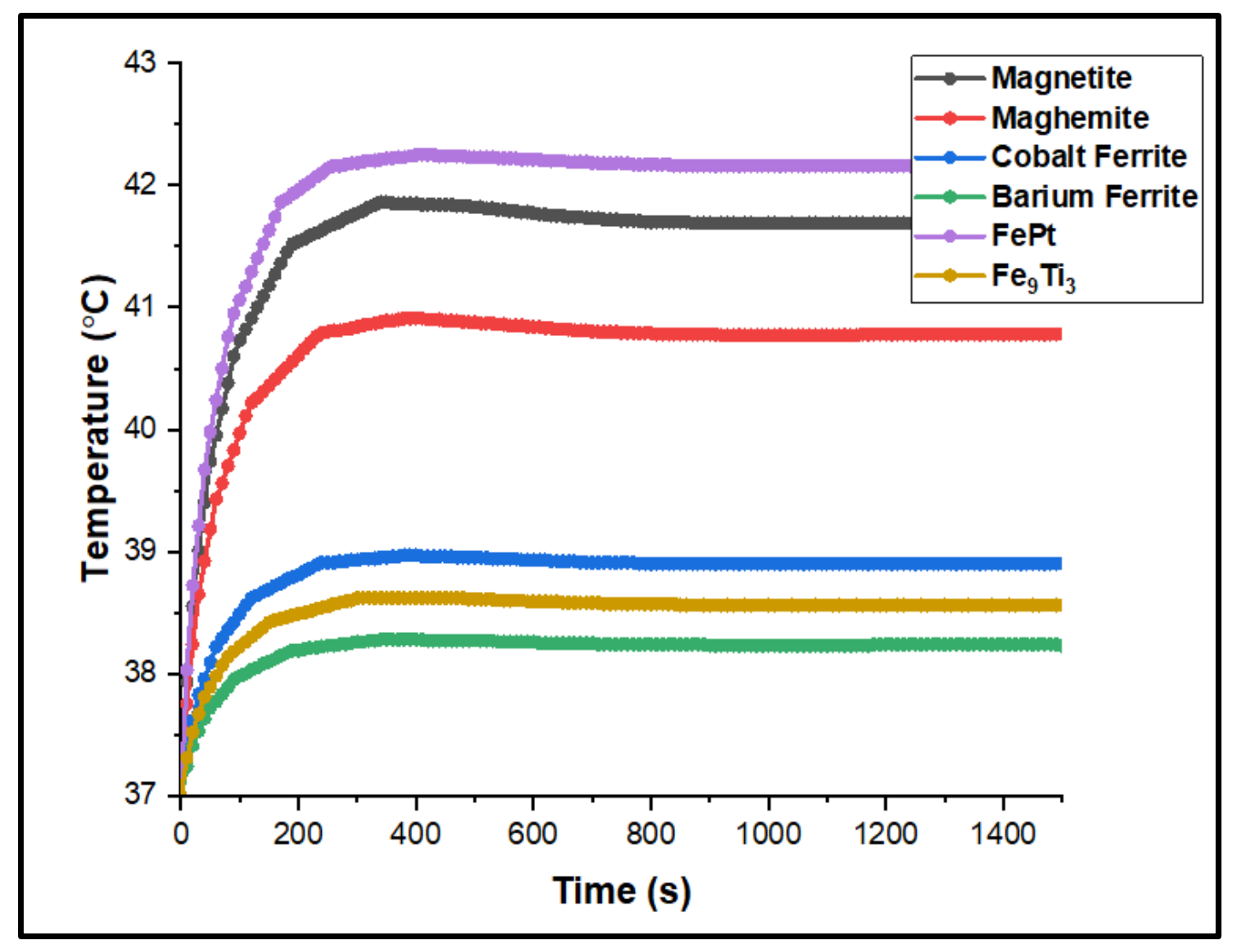

**Figure 2:** Temperature Progression at Tumor for all MNPs.

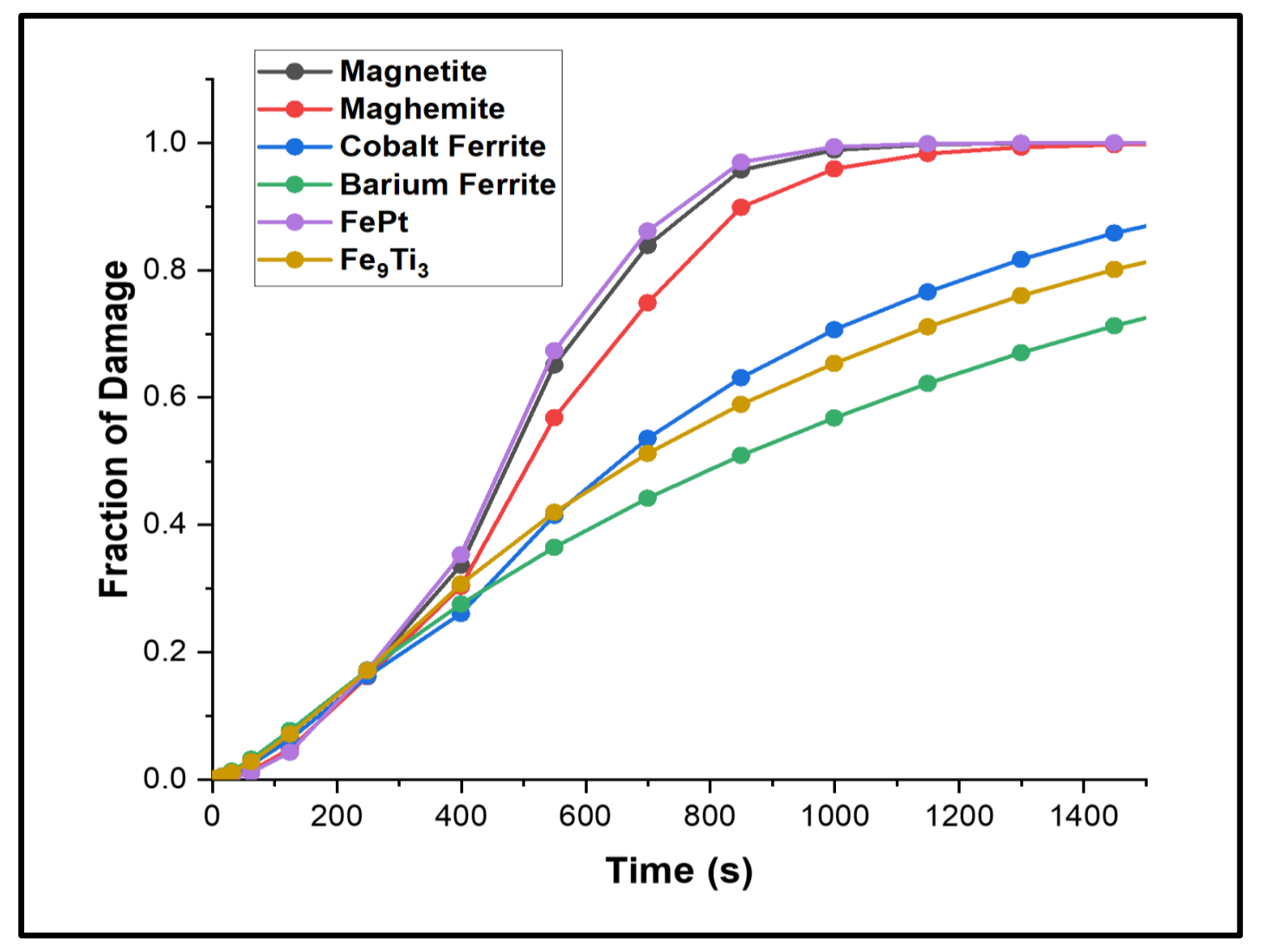

**Figure 3:** Fraction of Tumor Damage at a fixed dosage 1.5 kg/m³ for all MNPs.

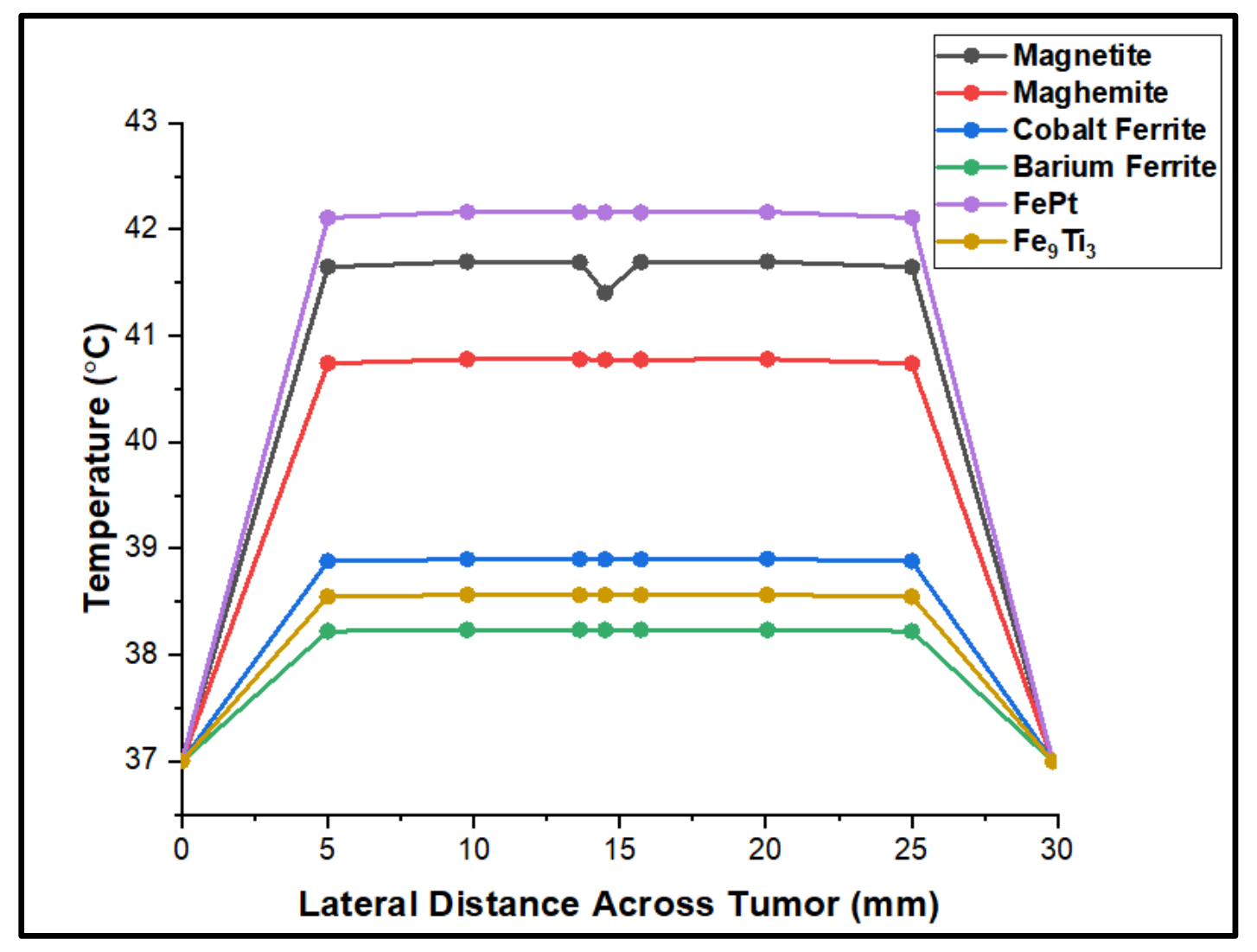

**Figure 4:** Temperature Distribution along tumor lateral distance for all MNPs.

**Table 1:** Physical and Magnetic Properties of Magnetic Nanoparticles [5,6,7].

| Magnetic Nanoparticle | Saturation Magnetization, Ms [kA/m] | Magnetic Anisotropy, K [kJ/m³] | Specific Heat Capacity, $c_{MNP}$ [J/kg·K] | Mass Density, $\rho_{MNP}$ [kg/m³] | Thermal Conductivity, $k_{MNP}$ [W/m·K] | Specific Loss Power, SLP [W/m³] |
|---|---|---|---|---|---|---|
| ***Magnetite*** | 446 | 9 | 670 | 5180 | 528 | $1.2\times10^9$ |
| ***Maghemite*** | 414 | 4.7 | 746 | 4600 | 528 | $9.25\times10^8$ |
| ***Cobalt Ferrite*** | 425 | 180 | 700 | 4907 | 528 | $4.65\times10^8$ |
| ***Barium Ferrite*** | 380 | 300 | 650 | 5280 | 528 | $3.03\times10^8$ |
| ***Iron Platinum*** | 1140 | 206 | 327 | 15200 | 528 | $2.2\times10^9$ |
| ***$Fe_9Ti_3$*** | 922.939 | 41 | 550 | 87664 | 528 | $2.5\times10^9$ |

**Table 2:** Physical and Physiological Properties of Liver Tumor and Healthy Tissue.

| Material (Liver) | Specific Heat Capacity [J/kg·K] | Mass Density [kg/m³] | Thermal Conductivity [W/m·K] | Frequency Factor [1/s] | Activation Energy [J/mol] |
|---|---|---|---|---|---|
| ***Tumor*** | 132 | 21500 | 71.0 | $7.39\times10^{39}$ | $2.577\times10^5$ |
| ***Healthy Tissue*** | 3540 | 1079 | 0.52 | $7.39\times10^{39}$ | $2.577\times10^5$ |

**Table 3:** Physical and Physiological Properties of Blood Vessel.

| Specific Heat Capacity [J/kg·K] | Mass Density [kg/m³] | Thermal Conductivity [W/m·K] | Electrical Conductivity [S/m] | Relative Permittivity |
|---|---|---|---|---|
| 3300 | 1100 | 0.543 | 0.667 | 1 |
| **Arterial Blood Temperature, $T_b$ [K]** | **Blood Perfusion Rate, $\omega_b$ [i = 1]** | **Metabolic Heat Source, $Q_i$ [i = 1]** | **Blood Perfusion Rate, $\omega_b$ [i = 2]** | **Metabolic Heat Source, $Q_i$ [i = 2]** |
| 310.15 | 0.0095 | 5790 | 0.003 | 700 |

**Table 4:** Results of Mesh Convergence Study for Magnetite.

| | Coarser | Coarse | Normal | Fine |
|---|---|---|---|---|
| **Degrees of Freedom** | 23578 | 44132 | 98592 | 208430 |
| **Average Temperature (℃)** | 41.78 | 41.74 | 41.69 | 41.67 |
| **Solution Time (s)** | 15 | 21 | 38 | 92 |

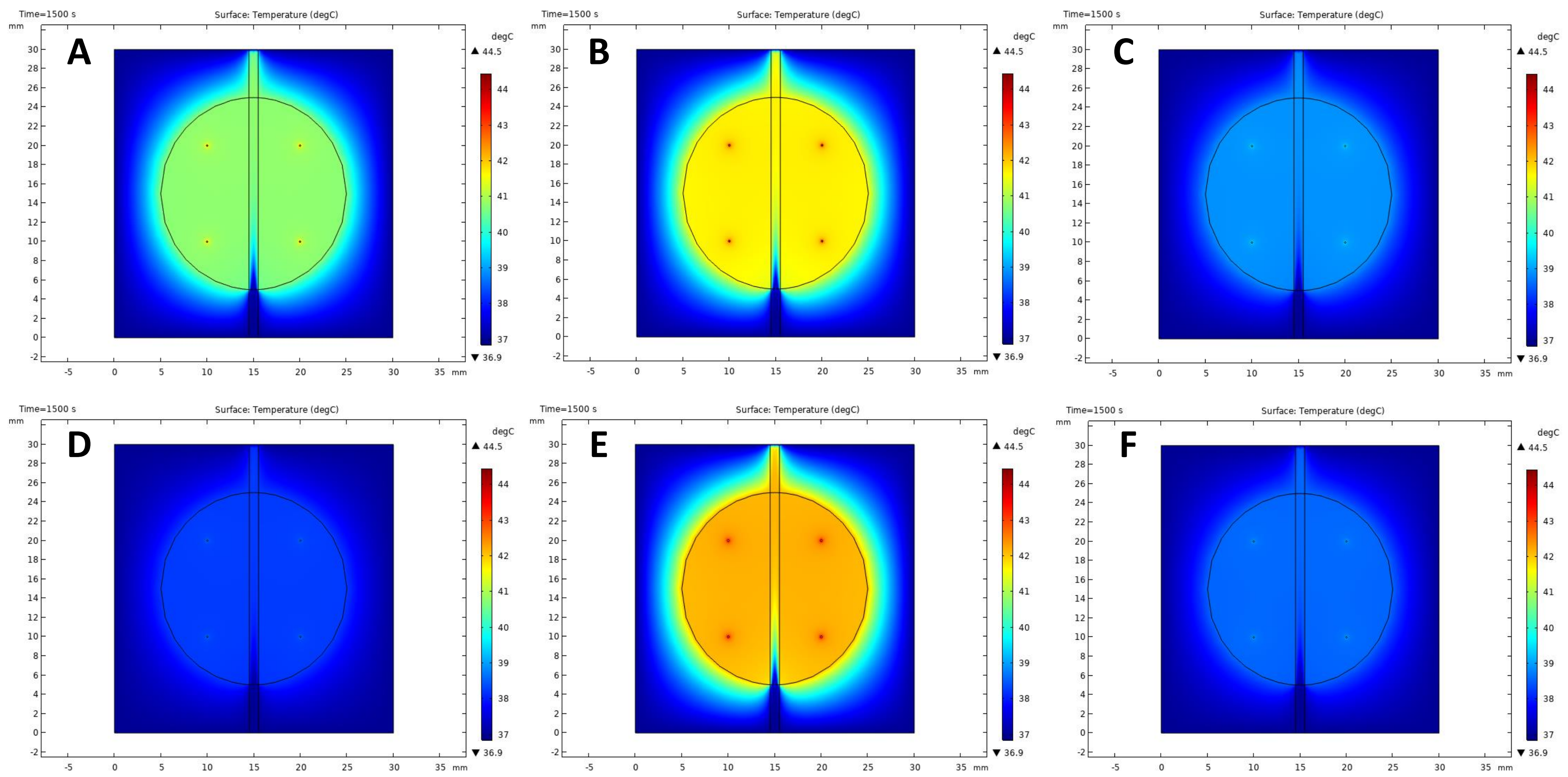

**Figure 5:** 2D Tumor Temperature Profile with 0.5 kg/m³ dosage for **A)** Maghemite, **B)** Magnetite, **C)** Cobalt Ferrite, **D)** Barium Ferrite, **E)** FePt, and **F)** $Fe_9Ti_3$ MNPs.

## V. Conclusion

- A two-dimensional model of the temperature profile illustrated that the temperature decreased abruptly at the center of the tumor, where the blood vessel is located.
- The cooling effect of the blood vessel was dependent on the blood velocity; thus, a higher blood velocity intensifies the cooling effect and thermal gradient of the tumor's temperature.
- Maghemite, magnetite, and iron platinum achieved maximum temperatures of 42.43℃, 42.76℃, and 44.44℃, respectively, which satisfies the desired temperature for magnetic hyperthermia treatment.
- In contrast, the cobalt ferrite, barium ferrite, and $Fe_9Ti_3$ MNPs achieved a slightly lower maximum temperature of 39.71℃, 38.75℃, and 39.23℃, respectively.
- As the particle dosage was increased, the fraction of tumor damage increased as well.
- Maghemite, magnetite, and iron platinum achieved approximately 100% of tumor damage within a shorter treatment time and lower dosage when compared to the results of cobalt ferrite, barium ferrite, and $Fe_9Ti_3$.
- Administering maghemite, magnetite, and iron platinum over cobalt ferrite, barium ferrite, or $Fe_9Ti_3$ would be optimal to achieve greater heat dissipation, a larger fraction of tumor damage, and shorter treatment duration.
- In an effort to validate the results provided in this study, a parametric mesh convergence study was conducted.
- Based on the results, there was no large deviation among the temperature values leading to the conclusion that either mesh size was an appropriate choice.
- It was determined that the Normal mesh size used for this study was appropriate in producing an accurate set of results for both temperature and the fraction of damage.

## VI. References

**1.** Spirou, S., Basini, M., Lascialfari, A., Sangregorio, C., & Innocenti, C. (2018). Magnetic Hyperthermia and Radiation Therapy: Radiobiological Principles and Current Practice †. Nanomaterials, 8(6), 401. doi: 10.3390/nano8060401.

**2.** Giustini, Andrew J., et al. "Magnetic Nanoparticle Hyperthermia In Cancer Treatment." Nano LIFE, vol. 01, no. 01n02, 2010, pp. 17–32. US National Library of Medicine National Institutes of Health, doi:10.1142/s1793984410000067.

**3.** Habib, A. H., et al. "Evaluation of Iron-Cobalt/Ferrite Core-Shell Nanoparticles for Cancer Thermotherapy." Journal of Applied Physics, vol. 103, no. 7, 2008, doi:10.1063/1.2830975.

**4.** Q. A. Pankhurst, J. Connolly, S. K. Jones, and J. Dobson, J. Phys. D 36, R167 2003.

**5.** Rosensweig, R.e. "Heating Magnetic Fluid with Alternating Magnetic Field." Journal of Magnetism and Magnetic Materials, vol. 252, 2002, pp. 370–374., doi:10.1016/s0304-8853(02)00706-0.

**6.** Habib, A.H., Ondeck, C.L., Chaudhary, P., Bockstaller, M.R., & McHenry, M.E. (2008). Evaluation of iron-cobalt/ferrite core-shell nanoparticles for cancer thermotherapy. Journal of Applied Physics, 103. doi: 10.1063/1.2830975.

**7.** Maenosono and S. Saita, IEEE Trans. Magn. 42, 1638 (2006).

## VII. Acknowledgements

The author would like to extend his gratitude to his faculty advisor, Dr. Huseyin Ucar, who has been an outstanding mentor throughout this research. Dr. Ucar's guidance, patience, encouragement, and understanding of the material has served a pivotal part in the success of this research. The author would also like to express his sincere gratitude to his family for their continued support, advice, and encouragement as he advanced through his undergraduate studies and research. He would also like to thank the CPP Student RSCA Conference for the opportunity to showcase his research.